ELSEVIER

Chemical Engineering Science 63 (2008) 1081–1091

Chemical Engineering Science

www.elsevier.com/locate/ces

Liquid water transport in a mixed-wet gas diffusion layer of a polymer electrolyte fuel cell

Puneet K. Sinha, Chao-Yang Wang*

Electrochemical Engine Center (ECEC), and Department of Mechanical and Nuclear Engineering, The Pennsylvania State University, University Park, PA 16802, USA

Received 13 August 2007; received in revised form 30 October 2007; accepted 4 November 2007
Available online 13 November 2007

Abstract

After PTFE treatment, a gas diffusion layer (GDL) of a polymer electrolyte fuel cell (PEFC) features mixed wettability, which substantially impacts liquid water transport and associated mass transport losses. A pore-network model is developed in this work to delineate the effect of GDL wettability distribution on pore-scale liquid water transport in a GDL under fuel cell operating conditions. It is found that in a mixed-wet GDL liquid water preferentially flows through connected GDL hydrophilic network, and thereby suppresses the finger-like morphology observed in a wholly hydrophobic GDL. The effect of GDL hydrophilic fraction distribution is investigated, and the existence of an optimum hydrophilic fraction that leads to the least mass transport losses is established. The need for controlled PTFE treatment is stressed, and a wettability-tailored GDL is proposed.

Keywords: Polymer electrolyte fuel cell; Mixed wettability; Gas diffusion layer; Liquid water transport; Pore-network modeling

1. Introduction

Owing to their high energy efficiency, low noise, and minimal pollution, fuel cells are widely regarded as 21st century energy-conversion devices for automotive, stationary and portable applications. Among them, the polymer electrolyte fuel cell (PEFC) has emerged as the most promising power source for a broad range of applications. PEFC is of a layered structure consisting of: a membrane electrode assembly (MEA) comprising a proton exchange membrane sandwiched between two catalyst layers (CL), two porous gas diffusion layers (GDL), and two bipolar plates with embedded gas channels. Protons and electrons produced by hydrogen oxidation reaction (HOR) in the anode CL flow through the membrane and the external circuit, respectively, and participate in the oxygen reduction reaction (ORR) in the cathode CL to generate water and waste heat.

Despite tremendous progress in overall cell performance has been made in the past decade, a pivotal performance/durability limitation in PEFCs centers on the transport of product liquid water and resulting flooding in the constituent components. Liquid water blocks reactant transport through the GDL, and incurs mass transport losses by hindering oxygen transport to the active reaction sites in the CL. The GDL, thus, plays a crucial role in the water management which requires a delicate balance between membrane hydration and water removal from the CL and GDL.

Carbon-fiber based porous materials, namely non-woven and woven carbon paper and carbon cloth with a thickness of $\sim 200\,\mu m$, are typically used for the PEFC GDL owing to their high porosity ($\sim 70\%$ or higher) and good electrical/thermal conductivity. SEM micrographs of a carbon paper and a carbon cloth are shown in Fig. 1. To facilitate liquid water removal from GDL, the GDL is treated with PTFE with loading varying from 5 to 30 wt% in order to induce and/or enhance hydrophobicity (Mathias et al., 2003). However, the wide range of wetting characteristics of carbon-based materials (Weber et al., 2004) as well as possible anomaly in the PTFE treatment renders part

* Corresponding author. Tel.: +1 814 863 4762; fax: +1 814 863 4848.
E-mail address: cxw31@psu.edu (C.-Y. Wang).

0009-2509/$ - see front matter © 2007 Elsevier Ltd. All rights reserved.
doi:10.1016/j.ces.2007.11.007

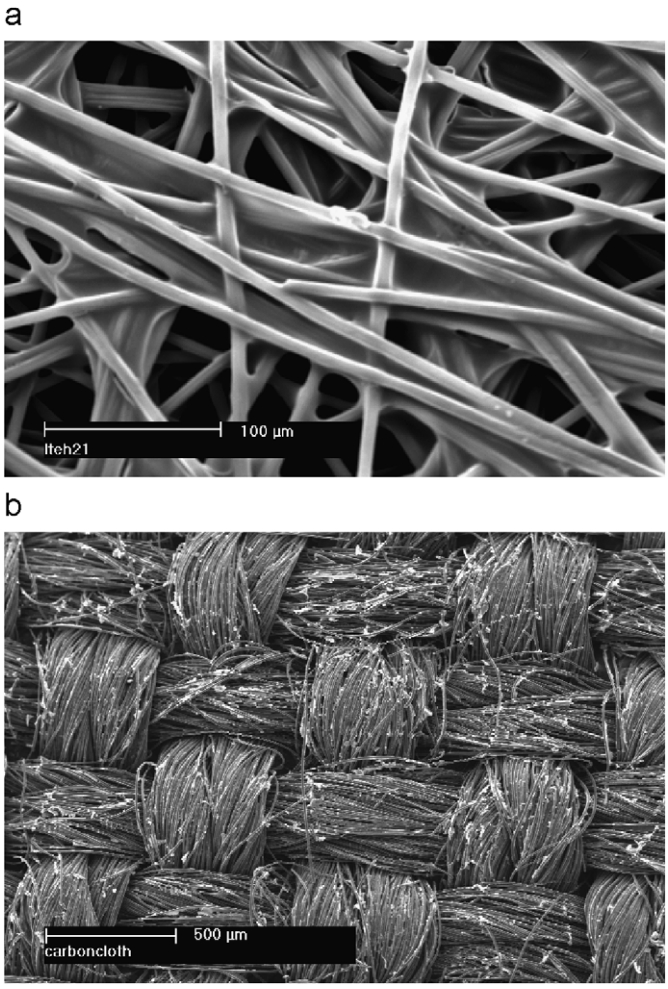

Fig. 1. SEM images of: (a) carbon paper and (b) carbon cloth GDLs.

of the GDL pores hydrophilic. Furthermore, surface defects, impurities, and ageing of the GDL might lead to a reduction in hydrophobicity, thereby causing mixed wettability surface characteristics. Recent experimental investigations (Gostick et al., 2006a) further confirm the mixed-wetting characteristics of GDLs.

While considerable research efforts, both numerical and experimental (Wang, 2004; Sinha et al., 2007), have been expended to delineate liquid water transport in a PEFC GDL and its effect on PEFC performance, the present theoretical understanding of liquid water transport is limited to a GDL with homogeneously hydrophilic or hydrophobic wetting characteristics. Existing theoretical models follow the macroscopic approach based on two-phase Darcy's law to investigate liquid water transport in PEFC. The two-phase Darcy's law inherently assumes that the liquid water transport is a compact process whereby the two-phase interface advances linearly with the total amount of injected fluid. Recently, Sinha and Wang (2007) delineated the pore-level physics of liquid water transport in a homogeneously hydrophobic GDL and showed that under realistic PEFC operating conditions (Ca $\sim 10^{-8}$), liquid water transport is governed by capillary fingering. Their investigation showed that liquid water enters the GDL in the form of fingers dominated by capillary forces. The majority of fingers encounter dead ends, and only few liquid water clusters breaks through the GDL–channel interface. These continuous clusters thus provide stable locations for water shadding from the GDL–channel interface, in consistency with transparent fuel cell observations (Yang et al., 2004; Zhang et al., 2006). Additionally, in their work crossover from fractal capillary fingering regime to compact invasion was observed at Ca $\sim 10^{-4}$ that is equivalent to unrealistically high 10^4 A cm^{-2} current density operation. Therefore, the two-phase Darcy's law based macroscopic treatment is inappropriate to describe liquid water transport in a homogenously hydrophobic GDL. However, the effect of wettability distribution on liquid water transport in a GDL was not probed. Few researchers (Weber et al., 2004; Nam and Kaviany, 2003; Pisani et al., 2002) have considered the GDL as partially hydrophilic. Weber et al. (2004) have taken mixed wettability of GDL into account via a composite contact angle as a function of the fraction of hydrophilic pores, f. They computed the maximum power and limiting current as functions of the fraction of hydrophilic pores, f, in GDL and showed the existence of an optimum value of f that leads to maximum limiting current and power. However, underlying liquid water transport mechanisms in a mixed-wet GDL were not studied.

In the last decade, the effect of wettability alteration and spatial wettability distribution on the multiphase flow characteristics has attracted much attention in the field of petroleum engineering and soil science. Kovscek et al. (1993) were the first to propose a pore-network model incorporating the wettability alteration in a porous medium. The wettability alteration model of Kovscek et al. (1993) is adopted by many researchers to investigate the effect of mixed wettability on transport properties of a general porous medium (Blunt, 1997, 1998; Dixit et al., 1999; Hui and Blunt, 2000; Piri and Blunt, 2002). Valvatne and Blunt (2004) delineated the underlying pore-scale processes governing oil recovery from mixed-wet sandstone. They further stressed the need of spatially correlated wettability distribution functions to quantitatively match experimental relative permeabilities of a mixed-wet porous medium. Al-Futaisi and Patzek (2004) investigated the effect of a wide range of advancing contact angles on the capillary pressure and relative permeability. Their results showed that the co-existence of hydrophilic and hydrophobic pores substantially affects relative permeability values. However, the effect of mixed wettability on phase distribution was not addressed in detail.

The present study aims to address the effect of mixed wettability on liquid water distribution in a GDL, and to answer the following questions:

(1) How does the co-existence of hydrophilic and hydrophobic pores in a GDL affect the fractal capillary fingering flow characteristics of liquid water transport?
(2) How can the PTFE treatment of a GDL be controlled to mitigate flooding and reduce associate mass transport losses during PEFC operation?

The paper is organized as follows: First, a pore-network model for a mixed-wet carbon paper GDL is described and the

algorithms to simulate two-phase flow in the generated pore network are presented. Then, the effect of GDL hydrophilic fraction and spatial wettability distribution on liquid water transport is elucidated. The role of controlled PTFE treatment on flooding mitigation is discussed, and a wettability-tailored GDL incurring the least mass transport losses is proposed.

2. Pore-network model

2.1. GDL network structure

Randomly distributed fibers in a carbon paper GDL furnish highly disordered pore space topology; therefore, a high resolution, three-dimensional image would be required to construct a topologically equivalent pore-network structure. As a first attempt, however, the methodology of Nam and Kaviany (2003) is followed in which carbon paper is regarded to consist of randomly stacked regular fiber screens that renders a three-dimensional random tetragonal pore-network structure with pores cubic in shape and throats of square cross section, as depicted in Fig. 2. The geometric and transport parameters used in the present PN model are summarized in Table 1. In the present study, pore and throat radii are assumed to have a cut-off log normal distribution. Various geometric parameters listed in Table 1 are chosen such that the porosity and absolute permeability fall in the range of a carbon paper GDL, as shown in Table 2. More development of topologically equivalent pore-network structure of a carbon paper GDL is currently underway. Main assumptions made in the PN model are: (1) while the radius of a throat serves to define its hydraulic conductance, the volume contributed by the throats is assumed to be small relative to the pore volume; (2) only one fluid can reside in a throat; (3) flow within a throat is assumed to be laminar and given by Hagen–Poiseuille law; (4) the resistance offered by a pore to flow is assumed to be negligible; and (5) fluids are assumed to be incompressible. A detailed discussion of these assumptions was presented in Sinha and Wang (2007), and therefore is not repeated here.

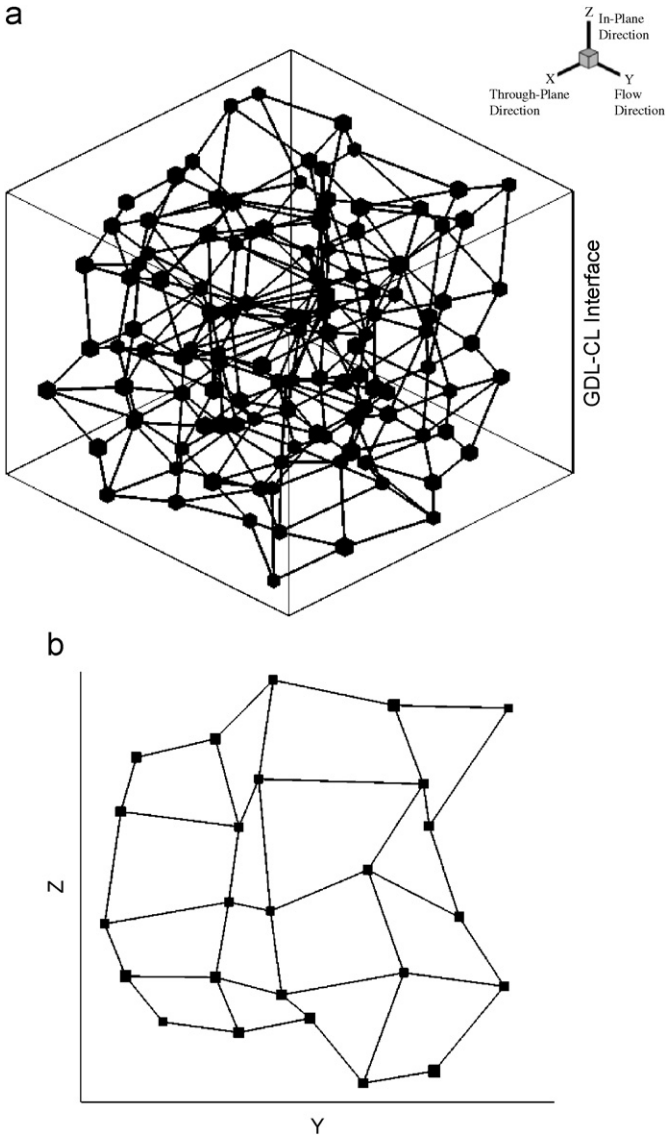

Fig. 2. Schematic of pore-network model for a carbon paper GDL: (a) 3D view and (b) 2D cross section showing the connectivity of pores in a plane.

2.2. Incorporation of mixed wettability

Since an accurate procedure to quantify the contact angle distribution inside the GDL is yet to be established, as a first approximation, random contact angle distribution is assumed, but correlated with the pore–throat sizes (larger throats are assigned larger contact angle). Plain GDL is dipped into aqueous PTFE suspension followed by heating and sintering. During this process, PTFE may not reach into very small pores leaving them hydrophilic. Hence the above-mentioned correlation of contact angle with pore throat sizes is considered. In the present work, contact angle is assumed to vary in the range of 60–120°. The upper limit of contact angle corresponds to a teflonized GDL pore, whereas the lower limit represents the contact angle of liquid water on an untreated carbon fiber (Yoon et al., 2007). It should be mentioned that surface roughness may alter the contact angle therefore it is assumed that contact angle may vary in the range of 60–90° in the hydrophilic pores and 90–120° in the hydrophobic pores of GDL. The complex behavior of liquid water at the mixed-wet GDL–channel interface, marked by pinning/unpinning of contact line as explained in Appendix A, is accounted for by assuming the GDL–channel interface to be hydrophobic with contact angle of the outlet throats varying in the range of 100–120°. Mixed wettability of a GDL is quantified by f, the fraction of pore throats that are hydrophilic. Hence $f = 0$ represents a hydrophobic GDL in which contact angle is distributed in a range of 90–120°. Results presented in this paper are based on the average of eight realizations of contact angle distribution with the other structural parameters kept the same.

2.3. Two-phase flow algorithm

For a realistic PEFC operation, capillary number is $\sim 10^{-8}$. Therefore, quasi-static description can be deployed to

Table 1
Pore network and transport parameters

Parameter	Value
Network Parameters	
Mean pore radius, r_{mean}	10 μm
Minimum pore radius, r_{min}	9 μm
Maximum pore radius, r_{max}	12.5 μm
Mean throat radius, $r_{th,mean}$	6 μm
Minimum throat radius, $r_{th,min}$	4 μm
Maximum throat radius, $r_{th,max}$	8.5 μm
Dimensions of PN structure	275 × 750 × 750 μm
Number of pores in x-direction	11
Number of pores in y-direction	30
Number of pores in z-direction	30
Cut-off log-normal distribution: for pore and throat size distribution	$f(r,\sigma_{nd}) = \frac{\sqrt{2}\exp\left[-0.5(\ln(r/r_{mean})/\sigma_{nd})^2\right]}{\sqrt{\pi\sigma_{nd}^2}r[\mathrm{erf}(\ln(r_{max}/r_{mean})/\sqrt{2\sigma_{nd}^2})-\mathrm{erf}(\ln(r_{min}/r_{mean})/\sqrt{2\sigma_{nd}^2})]}$
Std. deviation in pore and throat size distribution, σ_{nd}	1.0
Transport parameters	
Surface tension, σ	0.0725 N m^{-1}
Dynamic viscosity of liquid water	3.5×10^{-4} Pa s
Dynamic viscosity of air	2.0×10^{-5} Pa s

Table 2
Comparison of pore-network structural parameters with Toray® carbon paper

Parameter	Pore-network model	Toray® carbon paper
Mean pore diameter	20 μm	16–25 μm (Mathias et al., 2003)
Thickness	275 μm	110–370 μm
Porosity	62%	78–80% (without PTFE loading)
Absolute permeability (thickness direction)	5.6 D	5–10 D (Mathias et al., 2003)
Absolute permeability (in-plane direction)	6 D	5–12 D (Mathias et al., 2003)
Anisotropy factor (in-plane/through-plane)	1.07	1.3 (uncompressed) (Gostick et al., 2006b)

investigate liquid water transport in the GDL. Quasi-static description is applicable to flow in porous media at an infinitesimal flow rate, where the viscous pressure drop across the network is negligible and capillary forces completely control the fluid configuration. It should be mentioned that under realistic PEFC operating conditions, heat transfer across the GDL and ensuing phase change (Promislow et al., 2006; Wang and Wang, 2006) can substantially affect liquid water transport in a PEFC GDL. However, the present PN model is focused on elucidating flow dynamics of liquid water and hence is assumed isothermal and without phase change. The effect of temperature on pore-level liquid water transport mechanisms is left for future work.

Initially, all the pores and throats are completely filled with air and the inlet throats are connected to a reservoir of liquid water. Air pressure throughout the network is assumed to be constant, and equal to 1 atm. At each step of the quasi-static algorithm, a search is performed over all interface positions to determine the minimum capillary pressure that will allow liquid water to advance in the GDL. After updating liquid water pressure by this critical value, liquid water invades the connecting pore or throat and any subsequent pores or throats that can be accessed at the new liquid water pressure. At the end of each step trapped pores and throats are recognized using the extended Hoshen–Kopelman algorithm (Al-Futaisi and Patzek, 2003) and are excluded from the further calculation domain. Due to the co-existence of hydrophilic and hydrophobic pore–throats, various mechanisms governing local drainage and imbibition need to be taken into account. A brief description of various displacement mechanisms and their incorporation in the present model follows.

Liquid water invades the GDL when the pressure difference across an interface is larger that the capillary pressure of that interface. To avoid confusion in defining wetting and non-wetting phases for a mixed-wet GDL, we define capillary pressure as the difference between air and liquid water pressures, i.e.,

$$P_w - P_{\mathrm{air}} > P_c, \quad P_c = -\frac{2\sigma\cos\theta}{r}, \tag{1}$$

where P_w and P_{air} represent liquid water and air pressure, respectively, P_c the capillary pressure, r the radius of curvature at the interface, and θ the contact angle between liquid water and carbon fibers. As clear from Eq. (1), capillary pressure supports liquid water invasion when $\theta < 90°$, whereas it needs to be overcome for liquid water to invade further if $\theta > 90°$. Lenormand and Zarcone (1984) have shown that different mechanisms

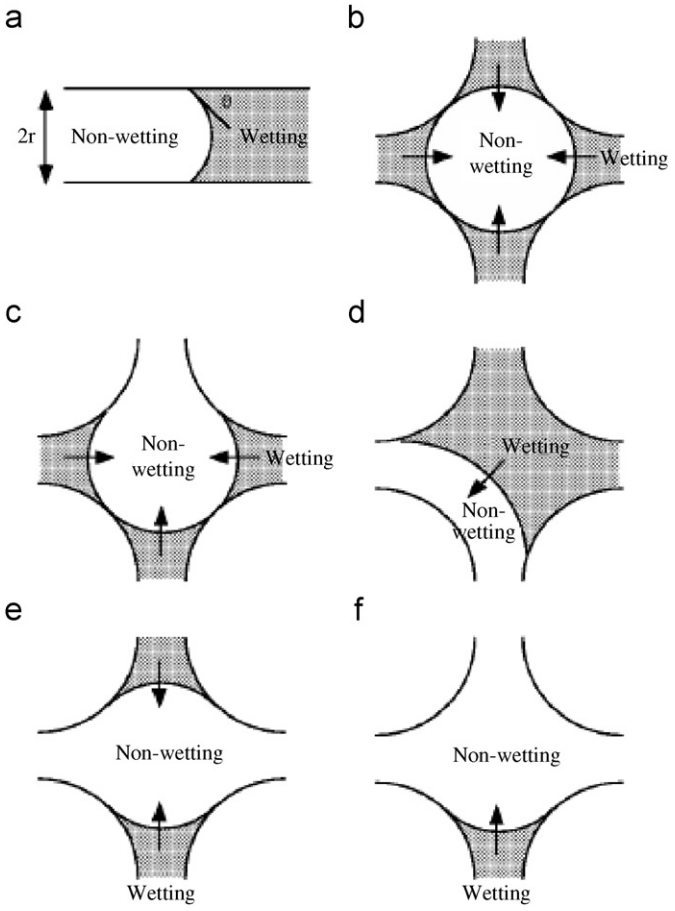

Fig. 3. Schematic representation of: (a) throat filling, and pore filling during imbibition (Mogensen and Stenby, 1998), (b) I_0 mechanism, not possible for incompressible fluids, (c) I_1 mechanism, (d) and (e) I_2 mechanism, and (f) I_3 mechanism.

govern liquid water invasion for drainage ($\theta > 90°$) and imbibition ($\theta < 90°$) processes. For clarity of presentation, the terms drainage and imbibition are used in the present work to represent liquid water invasion in hydrophobic and hydrophilic GDL fractions, respectively. For hydrophobic GDL volume, a pore will be automatically invaded once a connected throat is filled. Pore filling, however, is more complex for hydrophilic GDL volume, and is limited by the largest radius of curvature that can be achieved. This depends on the number of adjacent throats filled with non-wetting phase (air for hydrophilic GDL volume). A pore with coordination number z can thus be filled by $z-1$ possible events, I_1 to I_{z-1} as shown schematically in Fig. 3, each occurring at different capillary pressures. Blunt (1997) presented a parametric model to compute capillary pressure, $P_{c,n}$, and the mean radius of curvature, R_n, for an I_n mechanism:

$$P_{c,n} = \frac{2\sigma\cos\theta}{R_n} \quad \text{and} \quad R_n = \left(r_p + \sum_{i=1}^{n} b_i x_i r_{\text{th},i}\right), \quad b_1 = 0, \tag{2}$$

where r_p is the pore radius, b_i the input parameters, x_i the random numbers between 0 and 1, and $r_{\text{th},i}$ the radius of adjacent throats filled with non-wetting phase. As shown from Eq. (2), for I_1 mechanism, the mean radius of curvature, R_1, is minimum and is equal to pore radius, r_p, that makes I_1 the most favored event. With increase in the non-wetting phase filled neighboring throats, capillary pressure decreases making the hydrophilic pore invasion less likely. However, in the present work pore invasion is assumed to be governed only by pore radius, r_p, neglecting the exhaustive cooperative pore body filling mechanisms. It is found that hydrophobic outlet throats, as assumed in the present work, force complete filling of the connected hydrophilic GDL pore network in a mixed-wet GDL and therefore complex I_n events do not affect the steady-state saturation profiles in the mixed-wet GDL.

During imbibition, another displacement mechanism called snap-off may occur due to wetting films swelling to an extent that interface become unstable. Formation of wetting films along corners is governed by the Concus and Finn (1969) condition:

$$\theta + \alpha < 90°, \tag{3}$$

where θ and α are contact angle between wetting phase and solid matrix and half corner angle of a pore or a throat, respectively. Thus, a contact angle between liquid water and carbon fibers varying in the range of 60–120° and square cross section of pores and throats, as considered in the present work, suppress the existence of wetting films along the corners and hence the possibility of snap-off displacement mechanism. It should be mentioned that a small fraction of pores in the actual pore spaces of carbon paper may allow the formation of wetting films. Incorporation of wetting film flow, in accordance with the Concus and Finn (1969) condition, and snap-off mechanisms in a topologically equivalent pore-network structure of carbon paper is envisioned as a future extension of the present PN model.

The above-mentioned algorithm is continued till liquid water breaks out from the outlet face of the pore network.

2.4. Initial and boundary conditions

The GDL is initially saturated with air and the inlet face is in contact with a liquid water reservoir. A constant pressure boundary condition is imposed on the outlet face, whereas all other faces are subjected to no-flow boundary condition.

3. Results and discussion

In a real fuel cell operation, liquid water may appear at the GDL–channel interface in the form of liquid droplets or thin films, depending on the wettability of that interface. On a hydrophobic GDL–channel interface, as assumed in the present work, liquid water droplets grow to a critical size before being sheared away by the gas flow in the channel. Zhang et al. (2006) experimentally investigated the effects of gas flow rate on cell performance and GDL–channel interfacial droplet dynamics and showed the existence of substantial amounts of liquid water at the interface incurring mass transport losses at low gas flow rate. Sinha and Wang (2007) investigated the

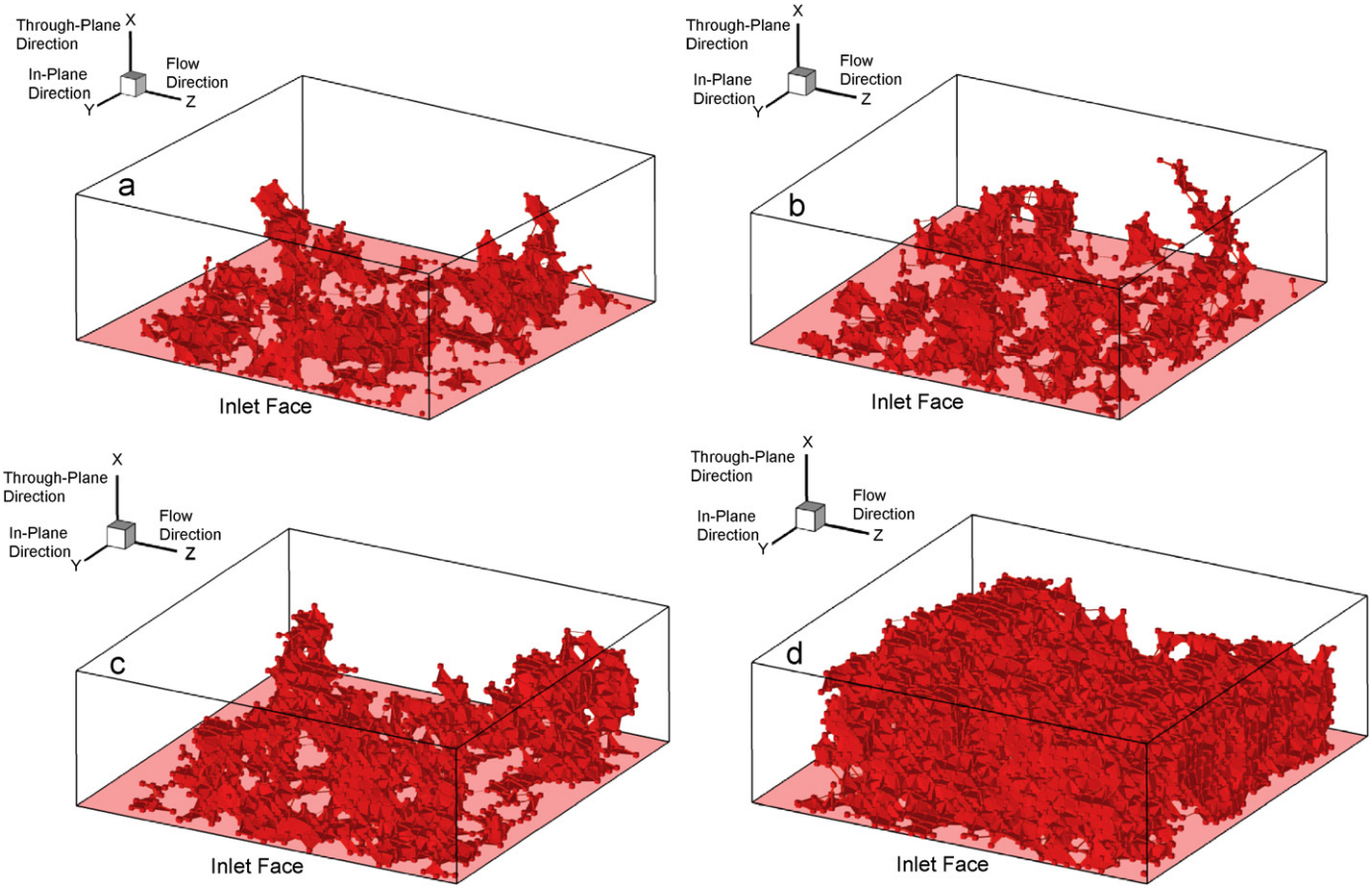

Fig. 4. Liquid water distribution in: (a) hydrophobic GDL with uniform contact angle of 110°, (b) hydrophobic GDL with contact angle distributed over the range of 90–110°, (c) mixed-wet GDL with $f = 10\%$, and (d) mixed-wet GDL with $f = 20\%$. Results are shown for a typical realization of contact angle distribution.

effect of GDL–channel interfacial water coverage on liquid water transport in a homogeneously hydrophobic GDL. In the present work, only zero GDL–channel interfacial water coverage is considered, which physically corresponds to sufficiently high gas flow rates in the gas channel.

3.1. Uniform distribution of GDL hydrophilic fraction

As mentioned in a previous section, GDL mixed wettability is quantified by GDL hydrophilic pore–throat fraction, f. First the effect of mixed wettability on liquid water transport is investigated with uniformly distributed hydrophilic pore–throat fraction along its thickness. Fig. 4 displays the steady-state liquid water distribution in different types of mixed-wet GDL for a typical realization of contact angle distribution. As shown in Fig. 4, the morphology of the liquid water front changes significantly with the hydrophilic fraction in a GDL. Fig. 4(a) shows fractal morphology of liquid water distribution in a homogenously hydrophobic GDL with contact angle of 110°. For GDL with $f = 0$, i.e., contact angle distribution in the range of 90–120°, the liquid water distribution, as shown in Fig. 4(b), features fractal morphology similar to homogenously hydrophobic GDL. For a GDL with non-zero hydrophilic fraction, liquid water preferentially flows through the connected hydrophilic pore network. As the hydrophilic fraction increases, the morphology crosses over from finger-like to piston-like compact shape, as shown in Fig. 4(c) and (d). The suppression of finger-shaped morphology in a mixed-wet GDL can be explained by Fig. 5. Fig. 5(a) schematically illustrates that for a gas–liquid interface to move in a hydrophobic GDL, the pressure difference across the interface must exceed the capillary pressure of the connecting throat. Thus, for the invasion of liquid water in pore 2, liquid pressure in pore 2, P_l^2, must be higher than air pressure. Suppose that the capillary pressure in the throat connecting pores 2 and 4 is low enough such that

$$P_l^2 - P_a^4 > P_c^{2,4}, \tag{4}$$

where P_a^4 and $P_c^{2,4}$ denote the air pressure in pore 4 and the capillary pressure of the throat connecting pores 2 and 4, respectively. If Eq. (4) is satisfied, the interface at the entrance of the throat connecting pores 2 and 4 grows unstable and liquid water will invade pore 4. However, if the throat connecting pores 2 and 3 is very narrow, as shown in Fig. 5(a), the interface cannot move from pore 2 into 3, resulting in a dead end to liquid water flow. On the other hand, Fig. 5(b) depicts the liquid water movement in a mixed-wet GDL with the throat connecting pores 2 and 3 becoming hydrophilic while the rest of the parameters remain the same as in Fig. 5(a). In order for

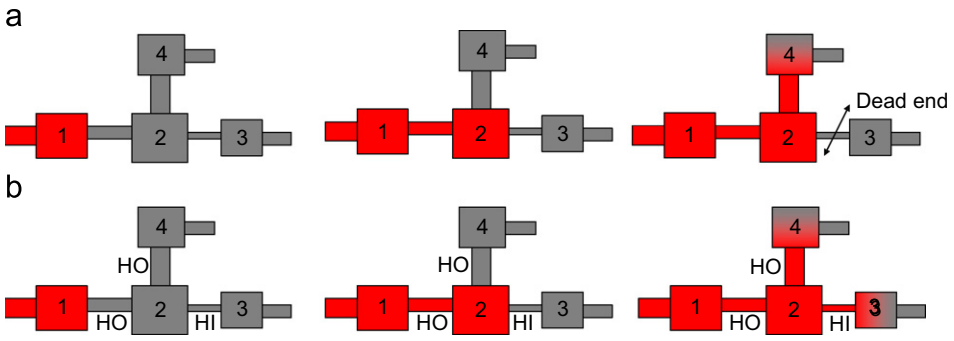

Fig. 5. Schematic representation of liquid water transport in: (a) a hydrophobic GDL and (b) a mixed-wet GDL, illustrating the suppression of dead ends in a mixed-wet GDL.

the liquid water interface to be stable at the entrance of the throat connecting pores 2 and 3, the following condition must be satisfied:

$$P_l^2 + |P_c^{2,3}| = P_a^3. \quad (5)$$

Again, when pore 2 is filled completely with liquid water, the liquid pressure in pore 2 is higher than air pressure as discussed earlier. This makes the interface unstable at the entrance of the throat connecting pores 2 and 3 irrespective of the connecting throat size. Thus, liquid water invades both the throats connecting pore 2 to pores 3 and 4 in the mixed-wet GDL, as shown in Fig. 5(b), which suppresses the occurrence of dead ends.

The pore-level events during liquid water invasion in a mixed-wet GDL can be further investigated by the variation of the inlet pressure, as shown in Fig. 6. Fig. 6(a) depicts variation of the gauge inlet pressure with average GDL liquid saturation for $f = 0.1$, for a typical realization of contact angle distribution. A positive gauge inlet pressure in Fig. 6(a) represents local drainage, i.e., liquid water invasion in the GDL region with $\theta > 90°$, whereas a negative value represents local imbibition, i.e., liquid water invasion in the GDL region with $\theta < 90°$. Higher density of local imbibition events marked by negative gauge inlet pressure in the beginning of invasion is due to the fact that connected hydrophilic pore network provides preferential path for liquid water transport. Once no hydrophilic pore–throat is available for invasion, liquid water invades the hydrophobic throat with the least capillary barrier pressure, resulting in a positive gauge inlet pressure. Fig. 6(b) depicts the variation of inlet gauge pressure for $f = 0.2$. As shown, the number density of local imbibition events substantially increases with GDL hydrophilic fraction, incurring substantially higher average liquid saturation in the GDL.

Fig. 7 shows the steady-state saturation profiles along the GDL thickness as a function of the hydrophilic fraction in a GDL averaged over eight realizations of contact angle distribution. The suppression of finger-like morphology in a mixed-wet GDL renders a change in saturation profile shape from concave, typical of fractal fingering, to convex, typical of stable front, with increase in hydrophilic fraction. The crossover from concave- to convex-shaped saturation profile, as clearly depicted in Fig. 7, lends support to the applicability of two-phase Darcy's law treatment to address liquid water transport

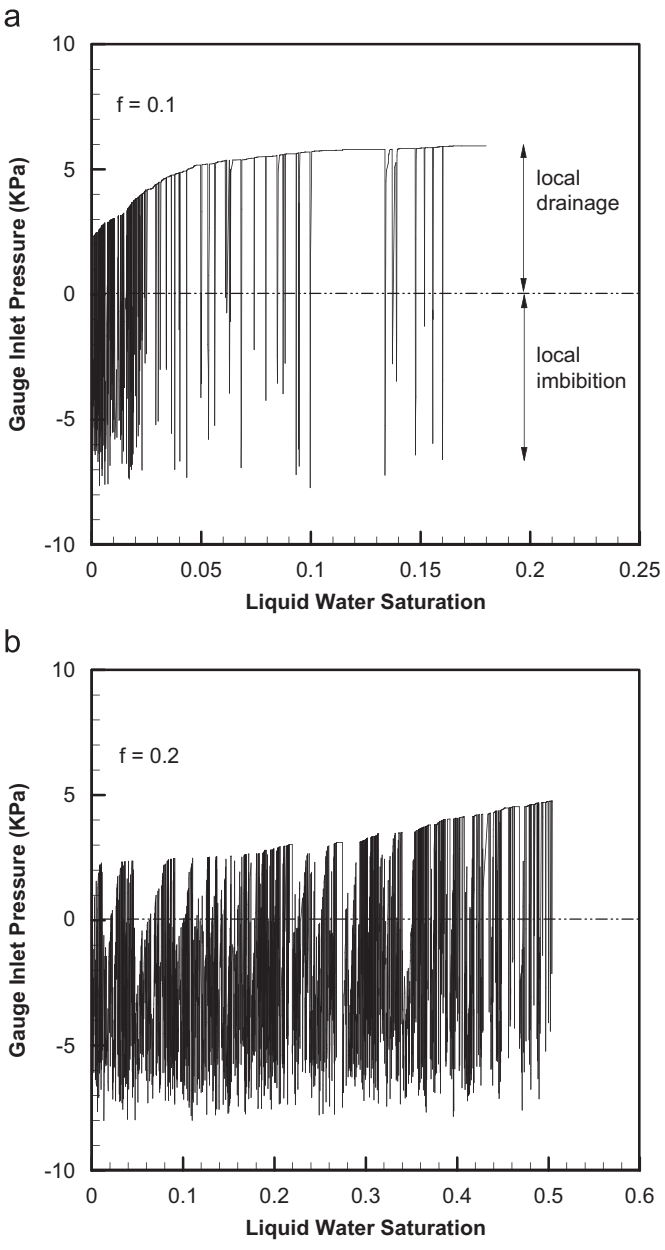

Fig. 6. Variation of inlet pressure variation with average liquid water saturation in mixed-wet GDLs for: (a) $f = 10\%$ and (b) $f = 20\%$.

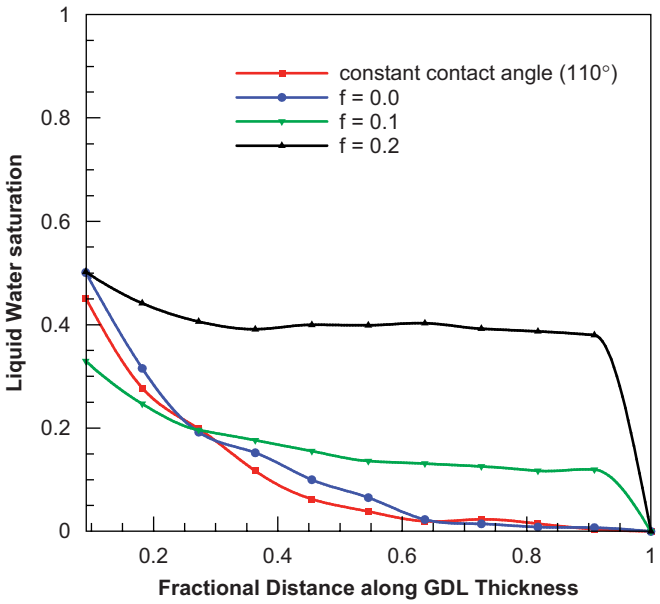

Fig. 7. Liquid water saturation profiles along GDL thickness as a function of the hydrophilic fraction *f*.

in a mixed-wet GDL with $f \geqslant 0.2$. In recent years, Ferer et al. (1993, 2003), among others, have conducted detailed investigations identifying the physics and parameters governing the crossover from capillary fingering to stable displacement regime. The present analysis shows that crossover from capillary fingering to stable displacement can occur due to contact angle variation even at very low capillary number. However, the most significant effect of wettability distribution on liquid water transport is reflected by the saturation level at the inlet face that physically corresponds to the GDL–CL interface. As shown in Fig. 7, the liquid saturation at the inlet face is smaller for a mixed-wet GDL with 10% hydrophilic fraction than that for a hydrophobic GDL. The lower saturation at the inlet face represents lower mass transport limitations due to GDL flooding. As the hydrophilic fraction in a mixed-wet GDL is further increased to 20%, the liquid saturation at the inlet face becomes higher, incurring significantly higher mass transport limitations to PEFC operation. In addition, higher hydrophilic fraction further increases average liquid water saturation in the GDL, as shown in Fig. 7. This demonstrates the existence of an optimum hydrophilic fraction in a GDL that yields the least mass transport limitations to PEFC operation.

3.2. Effect of GDL hydrophilic fraction distribution

The aforementioned analysis is carried out with hydrophilic fraction distributed uniformly along its thickness. To further investigate the effect of GDL hydrophilic fraction distribution on liquid water transport, a non-uniform distribution of GDL hydrophilic distribution along its thickness is considered, as shown in Fig. 8(a). The total hydrophilic fraction for the two distributions shown in Fig. 8(a) is 10%. Fig. 8(b) shows the steady-state liquid water distribution for a typical realization of

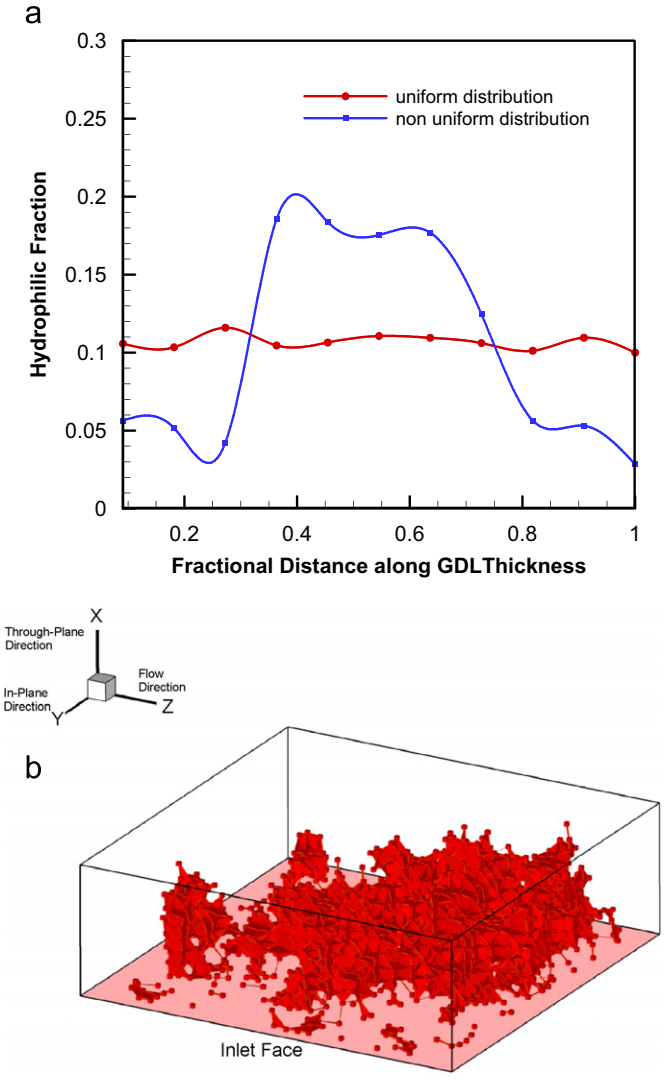

Fig. 8. Various distributions of GDL hydrophilic fraction considered in the present work. The total hydrophilic fraction is 10% for both the distributions and (b) liquid water distribution in a mixed-wet GDL with the non-uniform GDL hydrophilic fraction distribution. Distribution is for a typical realization of contact angle distribution.

the non-uniform hydrophilic fraction distribution in a mixed-wet GDL. Comparing Fig. 8(b) with Fig. 4(c) clearly shows that the distribution of GDL hydrophilic fraction substantially changes the liquid water distribution. The saturation profile along the GDL thickness, as shown in Fig. 9, more clearly depicts the effect of hydrophilic pore throat distribution in the GDL. The saturation profiles shown in Fig. 9 are averaged over eight realizations for contact angle distribution. Larger hydrophilic fraction in the inner layers of the GDL compared to the layers near inlet and outlet face renders substantially larger liquid saturation in the inner layers. The assumed non-uniform distribution entails lower saturation at the inlet face, as shown in Fig. 9. However, substantially higher liquid saturation in the inner layers makes the transport path for reactant transport more tortuous. Therefore, optimization of wettability distribution is critical to alleviate mass transport losses in PEFC operation.

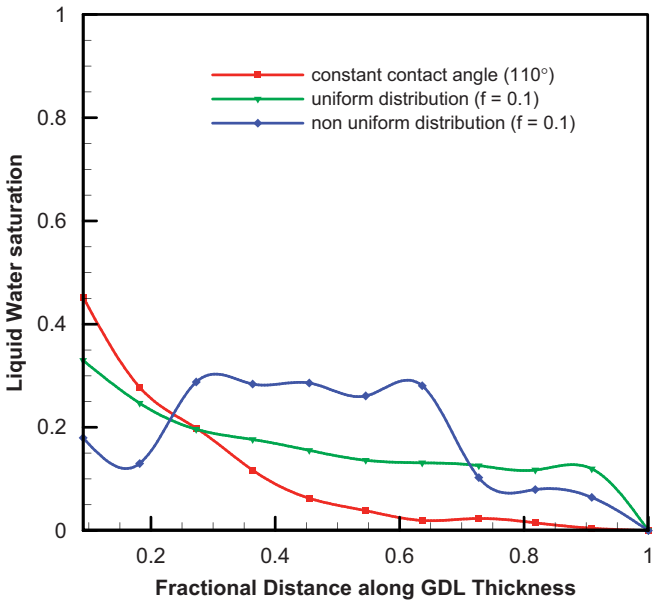

Fig. 9. Liquid water saturation profiles along GDL thickness as a function of GDL hydrophilic fraction distribution. Total GDL hydrophilic fraction is 10% for both distributions. For comparison the saturation profile for homogenously hydrophobic GDL is also shown.

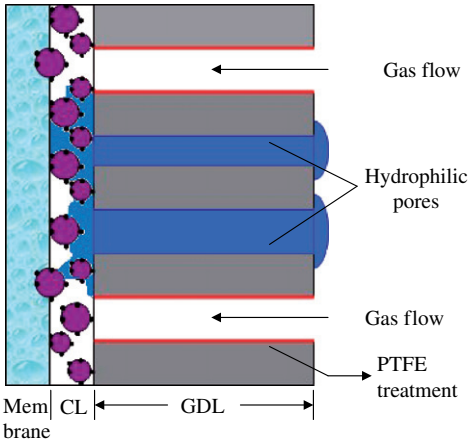

Fig. 10. Schematic representation of a wettability-tailored GDL.

A controlled PTFE treatment process that can yield a GDL shown schematically in Fig. 10 is desired. During PEFC operation, liquid water will occupy hydrophilic pore fraction, leaving the remaining pores for reactant transport and thereby will not incur significant mass transport losses.

4. Conclusions and future work

Elucidation of pore-level physics of liquid water transport in a mixed-wet GDL is essential not only to understand the role of mixed-wetting characteristics of a PEFC GDL in flooding phenomena but also to establish controlled PTFE treatment of GDL to mitigate flooding and associated mass transport losses. In the present work, a pore-network model is deployed to address the role of wettability distribution on flooding in a PEFC GDL. It is found that liquid water preferentially flows through the connected hydrophilic pore network of a mixed-wet GDL, suppressing finger-like liquid water morphology observed in a hydrophobic GDL. Crossover from fractal finger-like morphology to stable-front morphology is observed with increase in GDL hydrophilic fraction. The observed crossover, therefore, supports applicability of the two-phase Darcy's law based macroscopic treatment of liquid water transport in a mixed-wet GDL under realistic PEFC operating conditions ($Ca \sim 10^{-8}$). However, further research is required to develop an alternative macroscopic treatment to address capillary fingering phenomena encountered in a completely hydrophobic GDL. Also, it is found that there exists an optimum GDL hydrophilic fraction incurring the least mass transport losses. However, devising a coating process with controlled wettability is extremely challenging. In particular, GDL treatment with a conventional impregnation process with the PTFE water dispersion is extremely difficult to control, if not impossible. In recent years, novel hydrophobic coating processes based on plasma polymerization (Alyousef and Yao, 2006; Taniguchi and Yasuda, 2006; Yoon et al., 2007) were proposed that can alleviate many shortcomings of the conventional PTFE treatment. Masking the GDL surfaces during GDL treatment coupled with novel coating process may be a potential method to produce a mixed-wet GDL with separate transport paths for liquid water and gases as schematically shown in Fig. 10. However, further research is warranted to establish wettability-controllable coating processes for PEFC GDL.

It is imperative to develop experimental methods to quantitatively characterize the wettability of GDL pore walls which will allow further insight into the structure/wettability dependences of water management in PEFCs. A substantial challenge in deploying the aforementioned wettability-tailored GDL to real fuel cell applications lies in complex behavior of liquid water at the mixed-wet GDL–channel interface. To simplify the analysis, a hydrophobic GDL–channel interface is considered in the present work. Extensive research efforts are required to quantify liquid water dynamics at a mixed-wet GDL–channel interface, and to further incorporate it in the pore-network model to investigate the effect of liquid water coverage at the mixed-wet GDL–channel interface on flooding inside the GDL. In parallel, research efforts are currently underway to investigate effects of the presence of a land, GDL anisotropy, and various pore size distributions on liquid water motion in a mixed-wet GDL as well as to compute relative permeability and capillary pressure as functions of liquid saturation in a mixed-wet GDL.

Appendix A. Liquid water removal from mixed-wet GDL–channel interface

PEFC flooding and associated mass transport losses depend not only on the liquid water transport inside the GDL but also on the liquid water removal from the GDL–channel interface. Liquid water at the GDL surface may be present in the form of droplets or thin films depending on the wetting property of the interface as shown in Fig. 11(a) and (b). Detailed

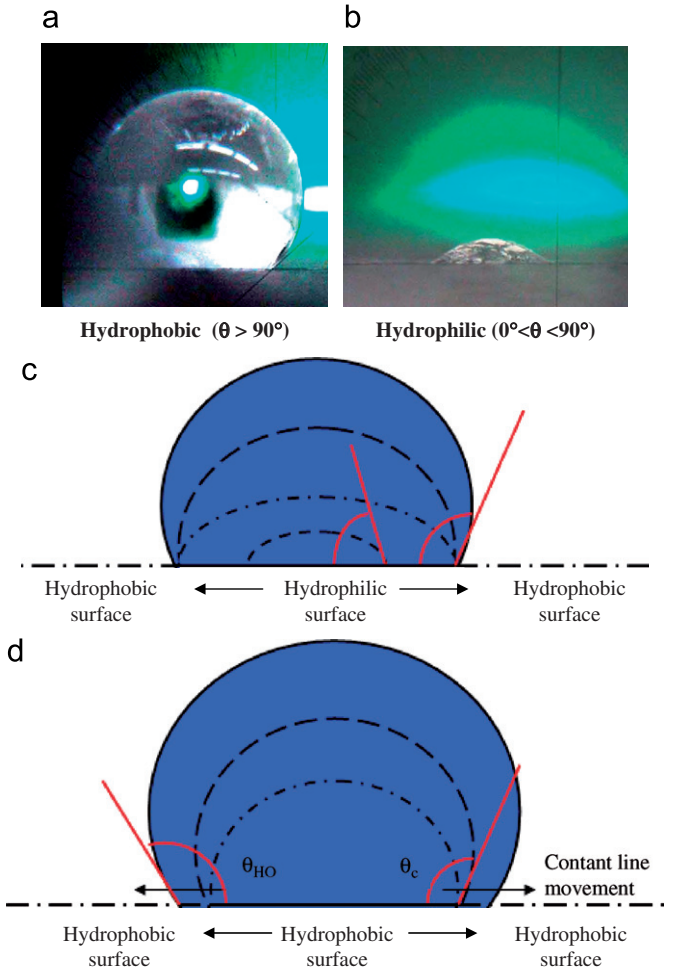

Fig. 11. Liquid water droplets on: (a) hydrophobic GDL surface; (b) hydrophilic GDL surface at 70 °C (Lim and Wang, 2003), (c) schematic representation of liquid water droplet growth with contact line pinning on a mixed-wet GDL surface, and (d) contact line unpinning once a critical contact angle is reached on mixed-wet GDL surface.

investigations have shown that on a hydrophobic GDL–channel interface liquid water droplets grow to a particular size before being sheared away by the gas flow in channel. The capillary pressure exerted by these droplets substantially increases liquid water saturation inside the GDL. As clear from Fig. 11(b), due to its curvature, a thin film of liquid water on a hydrophilic GDL–channel interface will exert a positive capillary pressure at the GDL–channel interface, and therefore will force 100% liquid water saturation inside the GDL.

However, liquid water removal from a mixed-wet GDL–channel interface is more complex, and can be envisioned as follows: Since liquid water preferentially flows through a connected hydrophilic pore network in a mixed-wet GDL, it breaks out from a hydrophilic pore at the interface, as shown schematically in Fig. 11(c). With constant injection rate of liquid water at the inlet face, the liquid film spreads over the hydrophilic GDL–channel interface via contact line movement. Once the liquid water film touches the interface of hydrophilic and hydrophobic sections of the GDL surface, pinning of contact line occurs. Liquid water movement with pinned contact line results in an increase in the contact angle that changes the liquid water morphology from a spread film to a droplet as shown schematically in Fig. 11(c). Such a newly formed droplet may be sheared away with gas flow. If the gas flow in the channel is not sufficient to shear away the droplet, the droplet contact angle will keep increasing till it reaches a threshold value, θ_c, that unpins the contact line. Further movement of contact line over the GDL–channel interface will cause enlargement of droplet size with change in contact angle according to the hydrophobic GDL surface, θ_{HO}. The enlargement of droplet size will continue until gas flow shears it or more hydrophilic channel wall wicks it away. The emergence and removal of liquid water from a mixed-wet GDL–channel interface, as schematically shown in Figs. 11(c) and (d), results in a positive capillary pressure at the breakout location, which entails complete filling of GDL hydrophilic fraction before liquid water emerges from the outlet face.

Contact line pinning/unpinning needs to be incorporated in the present pore-network model to address the effect of liquid water removal from a mixed-wet GDL–channel interface under realistic PEFC operating conditions. As a first attempt, however, the effect of liquid water removal from the mixed-wet GDL–channel interface can be addressed with the assumption of a completely hydrophobic GDL–channel interface. Hydrophobic outlet throats, as assumed in the present work, will ensure complete filling of available GDL hydrophilic fraction before liquid water breaks out from the outlet face.

References

Al-Futaisi, A., Patzek, T.W., 2003. Extension of Hoshen–Kopleman algorithm to non-lattice environments. Physica A 321, 665–678.

Al-Futaisi, A., Patzek, T.W., 2004. Secondary imbibition in NAPL-invaded mixed-wet sediments. Journal of Contaminant Hydrology 74, 61–81.

Alyousef, Y., Yao, S.C., 2006. Development of a silicon-based wettability controlled membrane for microscale direct methanol fuel cells. Microfluid Nanofluid 2, 337–344.

Blunt, M.J., 1997. Pore level modeling of the effects of wettability. Society of Petroleum Engineering Journal 2, 449–510.

Blunt, M.J., 1998. Physically based network modeling of multiphase flow in intermediate-wet porous media. Journal of Petroleum Science and Engineering 20, 117–125.

Concus, P., Finn, R., 1969. On the behavior of a capillary surface in a wedge. Applied Mathematical Sciences 63, 292–299.

Dixit, A.B., McDougall, S.R., Sorbie, K.S., Buckley, J.S., 1999. Pore-scale modeling of wettability effects and their influence on oil recovery. SPE Reservoir Evaluation & Engineering 2, 25–36.

Ferer, M., Sams, W.N., Geisbrecht, R.A., Smith, D.H., 1993. Crossover from fractal to compact flow from simulations of two-phase flow with finite viscosity ratio in two-dimensional porous media. Physical Review E 47, 2713–2723.

Ferer, M., Bromhal, G.S., Smith, D.H., 2003. Pore-level modeling of drainage: crossover from invasion percolation fingering to compact flow. Physical Review E 67, 051601-1–051601-12.

Gostick, J.T., Fowler, M.W., Ioannidis, M.A., Pritzer, M.D., Volfkovich, Y.M., Sakars, A., 2006a. Capillary pressure and hydrophilic porosity in gas diffusion layers for polymer electrolyte fuel cells. Journal of Power Sources 156, 375–387.

Gostick, J.T., Fowler, M.W., Pritzer, M.D., Ioannidis, M.A., Behra, L.M., 2006b. In-plane and through-plane permeability of carbon-fiber electrode backing layers. Journal of Power Sources 162, 228–238.

Hui, M.H., Blunt, M.J., 2000. Effects of wettability on three-phase flow in porous media. Journal of Physical Chemistry, B 104, 3833–3845.

Kovscek, A.R., Wong, H., Radke, C.J., 1993. A pore-level scenario for the development of mixed wettability in oil reservoirs. A.I.Ch.E. Journal 39, 1072–1085.

Lenormand, R., Zarcone, C., 1984. Role of roughness and edges during imbibition in square capillaries. Society of Petroleum Engineering Journal, 13264.

Lim, C., Wang, C.Y., 2003. Private communications.

Mathias, M.F., Roth, J., Fleming, J., Lehnert, W., 2003. Diffusion media materials and characterization. In: Lietsich, W., Lamm, A., Gasteiger, H.A. (Eds.), Handbook of Fuel Cells—Fundamentals, Technology and Applications, vol. 3, Wiley, Chicester, p. 517.

Mogensen, K., Stenby, E.H., 1998. A dynamic pore-scale model of imbibition. Transport in Porous Media 32, 299–327.

Nam, J.H., Kaviany, M., 2003. Effective diffusivity and water saturation distribution in single- and two-layer PEMFC diffusion medium. International Journal of Heat and Mass Transfer 46, 4595–4611.

Piri, M., Blunt, M.J., 2002. Pore-scale modeling of three-phase flow in mixed-wet systems. In: Proceedings of the SPE Annual Technical Conference and Exhibition, San Antonio, TX, September.

Pisani, L., Murgia, G., Valentini, M., Aguanno, B.D., 2002. A working model of polymer electrolyte fuel cells. Journal of Electrochemical Society 149, A898–A904.

Promislow, K., Stockie, J., Wetton, B., 2006. A sharp interface reduction for multiphase transport in a porous fuel cell electrode. Proceedings of Royal Society A 462, 789–816.

Sinha, P.K., Wang, C.Y., 2007. Pore-network modeling of liquid water transport in gas diffusion layer of a polymer electrolyte fuel cell. Electrochimica Acta 52, 7936–7945.

Sinha, P.K., Mukherjee, P.P., Wang, C.Y., 2007. Impact of GDL structure and wettability on water management in polymer electrolyte fuel cells. Journal of Materials Chemistry 17, 3089–3103.

Taniguchi, A., Yasuda, K., 2006. Waterproofing of carbon paper by plasma polymerization. Journal of Applied Polymer Science 100, 1748–1753.

Valvatne, P.H., Blunt, M.J., 2004. Predictive pore-scale modeling of two-phase flow in mixed wet media. Water Resources Research 40, W07406.

Wang, C.Y., 2004. Fundamental models for fuel cell engineering. Chemical Reviews 104, 4727–4766.

Wang, Y., Wang, C.Y., 2006. A non-isothermal two-phase model for polymer electrolyte fuel cells. Journal of the Electrochemical Society 153, A1193–A1200.

Weber, A.Z., Darling, R.M., Newman, J., 2004. Modeling two-phase behaviors in PEFCs. Journal of Electrochemical Society 151, A1715–A1727.

Yang, X.G., Zhang, F.Y., Lubawy, A., Wang, C.Y., 2004. Visualization of liquid water transport in a PEFC. Electrochemical and Solid State Letters 59, A408–A411.

Yoon, G.H., Park, S.B., Kim, E.H., Oh, M.-H., Cho, K.-S., Jeong, S.W., Kim, S., Park, Y.-I., 2007. Novel hydrophobic coating process for gas diffusion layer in PEMFCs, Journal of Electroceramics, 10.1007/s10832-007-9321-1.

Zhang, F.Y., Wang, X.G., Wang, C.Y., 2006. Liquid water removal from a polymer electrolyte fuel cell. Journal of the Electrochemical Society 153, A225–A232.